VII International Conference on Computational Plasticity
COMPLAS 2003
E. Oñate and D. R. J. Owen (Eds)

WRINKLING PREDICTION IN SHEET METAL FORMING AND EXPERIMENTAL VERIFICATION

Timo Meinders*, Sid Selman, Eisso H. Atzema***, Han Huétink***

* University of Twente
Faculty of Engineering Technology
Applied Mechanics
P.O. Box 217
7500 AE Enschede, The Netherlands
e-mail: v.t.meinders@ctw.utwente.nl
j.huetink@ctw.utwente.nl
Url: http:/www.wb.utwente.nl

** Netherlands Institute for Metals Research
Rotterdamseweg 137
2628 AL Delft, The Netherlands

*** Corus Research Development & Technology
IJTC, Automotive Applications
P.O. Box 10000
1970 CA IJmuiden, The Netherlands
e-mail: eisso.atzema@corusgroup.com

Key words: Wrinkling prediction, sheet metal forming

Abstract. *In this work, the analysis of Hutchinson and Neale is used for wrinkling prediction. Under a number of assumptions, limitations and simplifications a wrinkling criterion with some restrictive applicability, is obtained. Unfortunately, Hutchinson analysis is limited to regions of the sheet that are free of any contact. When contact is taken into account the problem is further complicated. Consequently, a local indicator based on the change of curvatures under compressive stresses is developed. Both wrinkling indicators are used to drive the adaptive mesh refinement in order to be able to accurately spot wrinkling. The numerical results will be compared to those obtained through experimental testing. A number of hemispherical product samples have been used with various blank holder forces and drawn to different depths to capture the onset of wrinkling, its mode and location.*

1. INTRODUCTION

Wrinkling is often observed in sheet metal products. In fact, wrinkling is becoming an important failure mode in sheet metal forming mainly because of the trend toward thinner, high strength sheet metals. If we want to simulate the sheet metal forming process, it is therefore important to be able to capture wrinkling in a FE model.

In a numerical simulation, wrinkles can be detected by visual inspection of the deformed mesh, provided that this mesh is fine enough to allow a proper capture of the wrinkles. On the other hand a fine mesh means high computational costs. Therefore the objective is to drive local mesh refinement with wrinkling indicators, which allows us to spot the wrinkles properly while keeping the computational costs as low as possible.

In this work, the analysis of Hutchinson and Neale[2], which consists of formulating the problem within the context of plastic bifurcation theory for thin shell elements and its extension by Neale[3] to account for more general constitutive models, is used. Under a number of assumptions, limitations and simplifications a simple wrinkling criterion with some restrictive applicability, is obtained. The results are used to locally define a wrinkling indicator, which in turn is used to drive the local mesh refinement.

However, Hutchinson analysis is limited to contact free regions. Therefore, a different approach must be used in regions where contact applies. Consequently, an indicator based on the local change of curvatures has been developed by Selman[4,5,6].

In section 2, both wrinkling indicators will be further explained. Section 3 will give a numerical example of the performance of the wrinkling indicators driving the local mesh refinement. An experimental verification will be given in section 4. The paper is finalized with some concluding remarks.

2. WRINKLING INDICATORS

This section treats two kinds of wrinkling indicators, one that can be applied in contact free regions only, and one that can be applied in zones where contact applies.

2.1 Contact free wrinkling analysis

Hutchinson[1] has developed the basic theory of plastic buckling and relevant relations for the Donnell-Mushtari-Vlasov shallow shell theory. The application of this theory to sheet wrinkling was first carried out by Hutchinson and Neale[2] and is used in the present work. However, it should be stressed that a number of assumptions, limitations and simplifications are embedded in Hutchinson analysis. First, we consider a sheet element, which, in the current stage of forming, has attained a doubly curved state with principal radii of curvature and thickness, all assumed to be constant over the region of the sheet being examined for susceptibility to local wrinkling. It is also assumed that the stress state prior to wrinkling to be a uniform membrane state over the local region being examined for wrinkling. Although the analysis can account for any stress state, for simplicity it is assumed that the principal axes of this uniform membrane stress state coincide with the principal axes of curvature. Simplifications arise from the fact that the anticipated short-wavelength modes are shallow

and that they can be analyzed using DMV shallow shell theory. Finally, the investigation is limited to regions of the sheet that are free of any contact.

To determine the critical stress state for buckling that is needed in the definition of the wrinkling indicator, Hutchinson bifurcation functional is used. The analysis involves substituting the fields used to describe wrinkling into the bifurcation functional and integrating over the local area of the sheet over which the wrinkles develop. Buckling is possible when the associated functional F is nil.

$$F = \beta\, S\, t \left(\frac{\mathrm{t}}{\mathrm{l}}\right)^2 \boldsymbol{u}^{\boldsymbol{T}}\, \boldsymbol{M}\, \boldsymbol{u} \tag{1}$$

With

$$\boldsymbol{M} = \mathrm{f}\left(\frac{1}{R}, \lambda, \boldsymbol{L}\right) \tag{2}$$

With $\boldsymbol{u}$ the buckling displacement amplitude vector, λ the wave number, β a scalar depending on the value of λ, S the local area of the sheet over which wrinkles develop, R the radius of curvature and $\boldsymbol{M}$ a matrix depending on the local geometry and incremental moduli. To determine the critical stress values for which short wavelength buckling first occurs, the determinant of F with respect to the waveform parameters is minimized and the minimum is set to zero. The values of the waveform parameters so obtained describe the corresponding critical buckling pattern:

$$\left.\begin{aligned} det\, \boldsymbol{M} &= 0 \\ \frac{\partial\, det\, \boldsymbol{M}}{\partial \lambda_1} &= 0 \\ \frac{\partial\, det\, \boldsymbol{M}}{\partial \lambda_2} &= 0 \end{aligned}\right\} \Rightarrow \sigma_1^{cr}\ ,\ \sigma_2^{cr}\ ,\ \lambda_1^{cr}\ ,\ \lambda_2^{cr} \tag{3}$$

These equations are highly non-linear and are generally solved by the Newton Raphson process. However the equations simplify when it is assumed that the wrinkling is aligned with one of the principal directions, which is true in most cases. For example, when the wrinkles are perpendicular to the 1 direction, λ_2 and σ_2 will be zero, and λ_{1_cr} and σ_{1_cr} can be determined.

As said in the introduction, high strength materials have a higher potential for wrinkling. This can be shown as follows. Given a specific hardening law (f.e. Nadai or Swift), we can define a critical strain (related to the critical stress) which depends on the square root of the hardening parameter and linear with the thickness, see equation (4). High strength materials have a low n-value and are usually thinner which gives them a higher potential for wrinkling.

$$\varepsilon^{cr} = f\left(\sqrt{n}, \frac{t}{R}\right) \tag{4}$$

Using the wrinkling critical stress values, a wrinkling risk factor (perpendicular to the ith direction) can be defined as

$$f_\sigma = \frac{\sigma_i}{\sigma_i^{cr}} \qquad \text{with i = 1 or 2} \tag{5}$$

Therefore a wrinkling risk exists whenever f_σ is larger than 1. Obviously, the risk is more important with larger values of the risk factors.

2.2 Wrinkling analysis in contact regions.

First, the wrinkling indicator proposed by Nordlund (7) was considered for a wrinkling analysis in contact regions. The algorithm is based on the local value of the internal work to capture the initiation of wrinkling.

$$I = \int_V tr\{(\dot{\sigma} + tr(\mathbf{L})\,\sigma - \mathbf{L}\,\sigma)\mathbf{L}\}\,\mathrm{dV} = \int_V \dot{\mathbf{f}}^{\mathrm{b}}\mathbf{v}\,\mathrm{dV} + \int_{S_t} \dot{\mathbf{f}}^{\mathrm{s}}\mathbf{v}\,\mathrm{dS} \tag{6}$$

with ***L*** the velocity gradient. The formation of wrinkles is characterized by the occurrence of areas where the deformation is dominated by strong out of plane rotations. Therefore the internal work is mainly determined by the following equation if wrinkling occurs (for a detailed derivation, see[5]):

$$\int_V tr\left\{\sigma(\mathbf{W}\mathbf{W}^T)\right\}\mathrm{dV} \tag{7}$$

with ***W*** the spin tensor. However, during a single deep drawing step, in a shallow wrinkling situation the rotations are small to very small and the compressive stresses are one order lower than the tensile stresses in the wrinkling zone, which relax at the initiation of wrinkling. Therefore, the wrinkling indicator cannot be used as a proper driver for mesh refinement in case of shallow wrinkling.

Therefore, a new indicator had to be developed. This indicator is based on the change of curvatures (during a single deep drawing step) under compressive stresses. Taking the change of curvature instead of taking the curvature itself, filters out all changes in curvature that are not due to compressive stresses, such as those caused for example by the geometry of the tool and the die. The new wrinkling indicator in the i^{th}-principal direction is defined as

$$e_i^w = \frac{1}{A}\int\left(\frac{1}{R_i^{t+\Delta t}} - \frac{1}{R_i^t}\right)dA = \frac{1}{A}\int\frac{R_i^t - R_i^{t+\Delta t}}{R_i^t R_i^{t+\Delta t}}dA \qquad i = 1,2 \tag{8}$$

with i representing the principal curvature direction and R_i^t, $R_i^{t+\Delta t}$ are the radii of curvatures in the i-direction at the beginning and at the end of a given deep drawing step, respectively. The

principal directions (stress and curvature) are considered one at the time as is the case with Hutchinson approach, and the maximum change for each element is taken. Consequently, the wrinkling indicator value e^w is defined as the maximum of e_i^w, i.e.

$$e^w = max\,(e_i^w) \qquad i = 1,2 \tag{9}$$

The wrinkling indicator value e_i^w is only calculated for elements under compressive stresses in the 1 and/or 2 principal directions. The wrinkling risk factor can now be defined as:

$$f_{gw} = \frac{e^w}{e^{avr}} \tag{10}$$

where e^{avr} is the average value of e^w over all rotating elements.

Note that as for Hutchinson approach, the present indicator, from now on referred to as the geometric wrinkling indicator, is local and of a *posteriori* type, and is therefore determined at a very low computational cost.

3. NUMERICAL EXAMPLE

The performance of the wrinkling indicators to drive the local mesh refinement will be demonstrated with a deep drawing simulation of a hemispherical product, applying a low blankholder force. A low blankholder force is chosen to cause the product to wrinkle under the blankholder (double contact). The simulation is started with a mesh comprising 2050 elements, Figure 1a. After a punch stroke of 30 mm, the mesh refinement in the wall of the product is driven by the Hutchinson wrinkling criterion, Figure 1b. After a punch stroke of 60 mm, the elements under the blankholder are refined, driven by the geometric wrinkling indicator, Figure 1c. At the final stage (punch stroke of 100 mm), severe wrinkling is observed under the blankholder, Figure 1d.

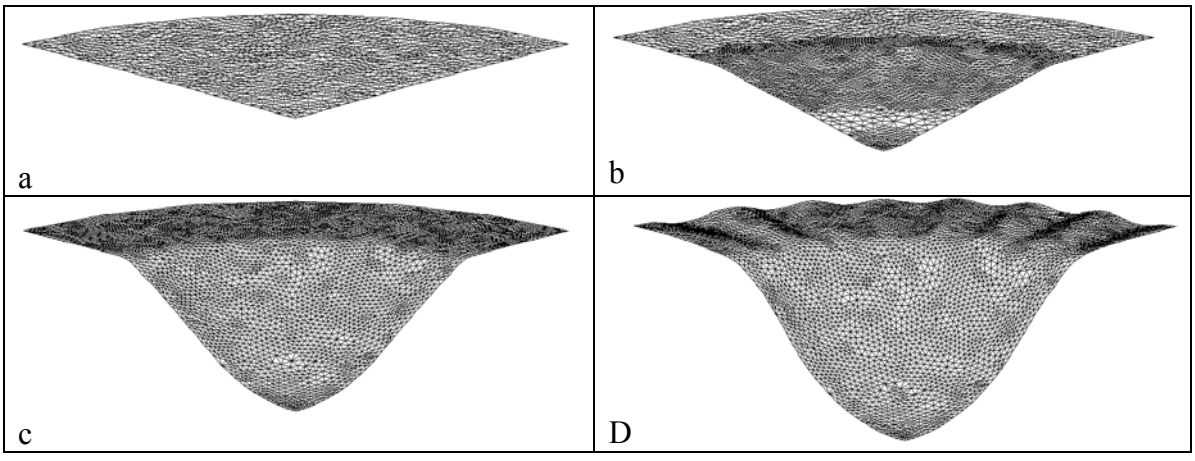

Figure 1. Mesh refinement, driven by both wrinkling indicators

4. EXPERIMENTAL VERIFICATION

To compare the numerical results with experiments, a hemispherical product has been used as a benchmark and a number of product samples stamped with various blank holder forces (BHF) and drawn to different depths to capture the onset of wrinkling, its mode and location.

4.1 Experimental procedure

The tests were held on a triple action 400 tonne hydraulic press (SMG) used in a dual action mode. The die was mounted on the ram and the punch mounted on the bed. The blankholder was supported by 8 pins resting on the cushion, with a load cell on top of each to measure the actual applied blank holder force. Moreover the pins were shimmed to achieve best possible load distribution under the blank holder. The blanks were cold-rolled galvanised IF steel with 560 mm diameter and 0.80 mm thickness. Only a small amount of lubricant was applied, since the amount of lubricant is known to affect the wrinkling behavior. The buckling waves were measured on a 3D coordinate measuring machine (CMM), Mitutoyo BH506 and corrected for the slight off-centre of the specimen by the proprietary Scan pack software. Then they were filtered via Fourier transformation, to remove long wavelength shape defects that were not of interest in this research.

4.2 Numerical and experimental results

The performance of the wrinkling prediction procedure with adaptive mesh refinement described in this work is compared with experimental data for a number of hemispherical product samples. The tool dimensions and material properties are given in Table 1.

Tool dimensions	(mm)	Material properties	
Punch radius	146.5	Elasticity modulus E	210 Gpa
Die radius	148.0	Poisson ratio ν	0.3
Die shoulder radius	20.0	Initial yield stress σ_0	172 Mpa
Blank diameter	560.0	Hardening parameter C	528 Mpa
Blank thickness	0.8	Hardening parameter n	0.225
		Lankford R_0	2.19
		Lankford R_{45}	1.72
		Lankford R_{90}	2.50

Table 1. Tool dimensions and material properties

A punch speed of 25 mm/s has been used. The friction coefficient is set to 0.1 in case a low blankholder force is used, in case a high blankholder force the friction coefficient is set to 0.16. The experiments and simulations will be compared with respect to the onset of wrinkling and the number of wrinkles. Experimentally, the onset of wrinkling is defined as the instant at which wrinkling becomes visible with the naked eye. The numerical onset of

wrinkling is defined as the instant at which the tangent in plot of the curvature versus time step becomes maximal, see Figure 2.

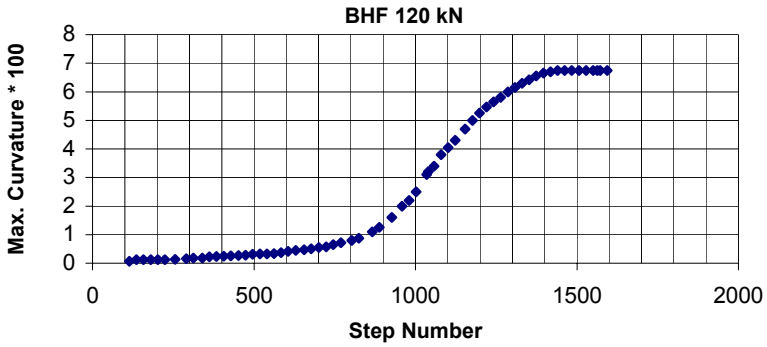

Figure 2. Maximum curvature versus. step number (BHF 120 kN).

The experimental and numerical results are summarized in Table 2 and Table 3. The experimental results are an average of a series of experiments[8]. In the simulations, only a quarter of the product is simulated to reduce the computation time; the number of wrinkles is high enough to produce only a small error.

BHF (kN)	120	150	200
Experimental Testing	27	27	0
Numerical Analysis	28	28	0

Table 2**.** Number of wrinkles.

BHF (kN)	120	150	200
Exp. Onset Draw Depth (mm)	101	107	Up to 250 (No Onset)
Num. Onset Draw Depth (mm)	96	104	Up to 250 (No Onset)

Table 3. Onset of wrinkling.

Regarding load cases 120 kN and 150 kN, the numerical prediction of the number of wrinkles is in good agreement with experimental results, see Table 2 and Table 3 (note: since only a quarter of the product is simulated, an uneven number of wrinkles can never be predicted). The onset of wrinkling is also in good agreement with experimental testing although in numerical analyses wrinkles start developing slightly before the experimental ones. It has also been observed that the numerical simulation tends to overestimate the

amplitude of the wrinkles. These observations are in accordance with earlier research on the same geometry[9,10].

Regarding the load case of 200 kN, in both the simulation and the experiment, no wrinkling occurred.

5. CONCLUSIONS

Hutchinson approach based wrinkling indicator that handles contact free wrinkling has been complemented with a new wrinkling indicator based on local curvature changes, which can be applied in regions with contact; i.e. the geometric wrinkling indicator. The main difference between these two wrinkling indicators is as follows. The Hutchinson approach based wrinkling indicator computes a risk factor prior to wrinkling, while the geometric wrinkling indicator comes into action only when a change in curvature under compressive stresses takes place. However, this is not much of a drawback, as this indicator is able to spot wrinkling at an early stage due to its high sensitivity to any change in the curvatures. A hemispherical product has been considered with a high and a low blank holder force to distinguish between contact free wall wrinkling and wrinkling with contact that takes place in the flange.

A hemispherical product has been used as a benchmark test with various BHF and drawn experimentally in a series of tests at different forming depths to spot the onset, location and mode of wrinkling. In comparing the numerical results with those obtained through experimental testing, a good agreement has been found in terms of location, onset and modes of wrinkling. However, the numerical analyses slightly overestimate the experimentally observed amplitudes of the wrinkles as well as it predicts an onset of wrinkling somewhat earlier than experimentally observed. This the makes numerical analysis conservative compared to experimental testing.

6. ACKNOWLEDGMENTS

This research was carried out under project number ME97033 in the framework of the Strategic Research program of the Netherlands Institute for Metals Research in the Netherlands (www.nimr.nl).

REFERENCES

[1] J.W. Hutchinson, Plastic buckling*, Adv. Appl. Mech*., **14**, p. 67-144, (1974)

[2] J.W. Hutchinson and K.W. Neale, Wrinkling of curved thin sheet metal, *Plastic Instability, J. Salencon (Ed.), Press Ponts et Chaussees,* p. 71-78, (1985)

[3] K.W. Neale, Numerical analysis of sheet metal wrinkling, *Numiform '89, Thompson et al (Eds.),* Balkema, Rotterdam, p. 501-505, (1989)

[4] A. Selman and T. Meinders and A.H. van den Boogaard and J. Huétink, Wrinkling prediction with adaptive mesh refinement*, 3rd ESAFORM Conference on Material Forming, Stuttgart, 11-14 April*, (2000)

[5] A. Selman and T. Meinders and A.H. van den Boogaard and J. Huétink, Comprehensive approach to wrinkling prediction analysis in thin sheet metal forming processes, *Submitted to Int. J. Num. Meth. Engng,* (2001)

[6] A. Selman and T. Meinders and A.H. van den Boogaard and J. Huétink , On Adaptive Mesh Refinement in Wrinkling Prediction Analysis*,* 5th *ESAFORM Conference on Material Forming, Krakow, 14-17 April*, (2002)

[7] P. Nordlund and B. Haggblad, Prediction of wrinkle tendencies in explicit sheet metal forming simulations, *Int. J. Num. Meth. Engng*, **40**, p. 4079-4095, (1997)

[8] A. Selman and E.H. Atzema and T. Meinders and A.H. van den Boogaard and J. Huétink, Wrinkling in sheet metal forming: experimental testing vs. numerical analysis, *accepted for publication in Int. J. of Forming Processes*, (2003)

[9] Medenblik and Liemburg, Persproeven ter controle van simulatie berekeningen secundaire plooivorming*, CorusRD&T internal report* 90428*,* (2000)

[10] R. ter Haar and E.H. Atzema, The impact of lubricant buffering on the operating window of deep drawing processes, *Proceedings of the 21st Biennial Congress of the Interantional DeepDrawing Research Group*, Ann Arbor, MI, USA, (2000)